JOURNAL OF NEUROPHYSIOLOGY
Vol. 76. No. 6. December 1996. *Printed in U.S.A.*

Perceptual and Motor Processing Stages Identified in the Activity of Macaque Frontal Eye Field Neurons During Visual Search

KIRK G. THOMPSON, DOUG P. HANES, NARCISSE P. BICHOT, AND JEFFREY D. SCHALL
Vanderbilt Vision Research Center, Department of Psychology, Vanderbilt University, Nashville, Tennessee 37240

SUMMARY AND CONCLUSIONS

1. The latency between the appearance of a popout search display and the eye movement to the oddball target of the display varies from trial to trial in both humans and monkeys. The source of the delay and variability of reaction time is unknown but has been attributed to as yet poorly defined decision processes.

2. We recorded neural activity in the frontal eye field (FEF), an area regarded as playing a central role in producing purposeful eye movements, of monkeys (*Macaca mulatta*) performing a popout visual search task. Eighty-four neurons with visually evoked activity were analyzed. Twelve of these neurons had a phasic response associated with the presentation of the visual stimulus. The remaining neurons had more tonic responses that persisted through the saccade. Many of the neurons with more tonic responses resembled visuomovement cells in that they had activity that increased before a saccade into their response field.

3. The visual response latencies of FEF neurons were determined with the use of a Poisson spike train analysis. The mean visual latency was 67 ms (minimum = 35 ms, maximum = 138 ms). The visual response latencies to the target presented alone, to the target presented with distractors, or to the distractors did not differ significantly.

4. The initial visual activation of FEF neurons does not discriminate the target from the distractors of a popout visual search stimulus array, but the activity evolves to a state that discriminates whether the target of the search display is within the receptive field. We tested the hypothesis that the source of variability of saccade latency is the time taken by neurons involved in saccade programming to select the target for the gaze shift.

5. With the use of an analysis adapted from signal detection theory, we determined when the activity of single FEF neurons can reliably indicate whether the target or distractors are present within their response fields. The time of target discrimination partitions the reaction time into a perceptual stage in which target discrimination takes place, and a motor stage in which saccade programming and generation take place. The time of target discrimination occurred most often between 120 and 150 ms after stimulus presentation.

6. We analyzed the time course of target discrimination in the activity of single cells after separating trials into short, medium, and long saccade latency groups. Saccade latency was not correlated with the duration of the perceptual stage but was correlated with the duration of the motor stage. This result is inconsistent with the hypothesis that the time taken for target discrimination, as indexed by FEF neurons, accounts for the wide variability in the time of movement initiation.

7. We conclude that the variability observed in saccade latencies during a simple visual search task is largely due to postperceptual motor processing following target discrimination. Signatures of both perceptual and postperceptual processing are evident in FEF. Procrastination in the output stage may prevent stereotypical behavior that would be maladaptive in a changing environment.

INTRODUCTION

It is well known that the amount of time taken to generate a saccade to a peripheral target varies across trials, but this variability cannot be accounted for by sensory and motor transduction delays plus transmission times through visuomotor pathways (Carpenter 1981). The delay and variation of behavioral reaction times seems to be due to decision processes in the brain (Carpenter and Williams 1995; Luce 1986). However, the nature of these decision processes is very poorly understood. Investigations of the oculomotor system can provide useful information on this question, because the key areas involved in saccade generation and the signals generated by neurons in those areas have been characterized.

The frontal eye field (FEF) is an area in frontal cortex that lies at the interface between visual processing and motor production (reviewed in Bruce 1990; Goldberg and Segraves 1989; Schall 1991c). We have been investigating the neural activity in the FEF associated with saccade target selection during visual search (Schall and Hanes 1993; Schall et al. 1995a). The activity of most FEF neurons initially does not discriminate whether the target or distractors of a search array fall in the response field. However, the activity evolves to signal the location of the target before the saccade is initiated through suppression of the activity evoked by distractors.

Because FEF is commonly regarded as playing a central role in generating saccades, it is plausible if not likely that the time that FEF cells discriminate the location of the target predicts the time of saccade initiation. In other words, the variability in the duration of perceptual processing is the source of reaction time variability. We refer to this as the perceptual stage hypothesis. The alternative hypothesis is that the time of target discrimination reflected in FEF does not predict the reaction time. In this latter case, other processes related specifically to saccade generation would be responsible for the variability in reaction time observed from trial to trial. We will refer to this as the motor stage hypothesis. Hybrid hypotheses are clearly plausible, but we choose to consider the two most distinct alternatives. These alternative hypotheses can be evaluated by examining the relationships between the time of stimulus presentation, the time of target discrimination, and the time of movement initiation as illustrated in Fig. 1.

The purpose of this study was to evaluate whether the time course of target discrimination evident in the activity of visually responsive FEF neurons predicts the time of saccade initiation. We unexpectedly found that the time taken for

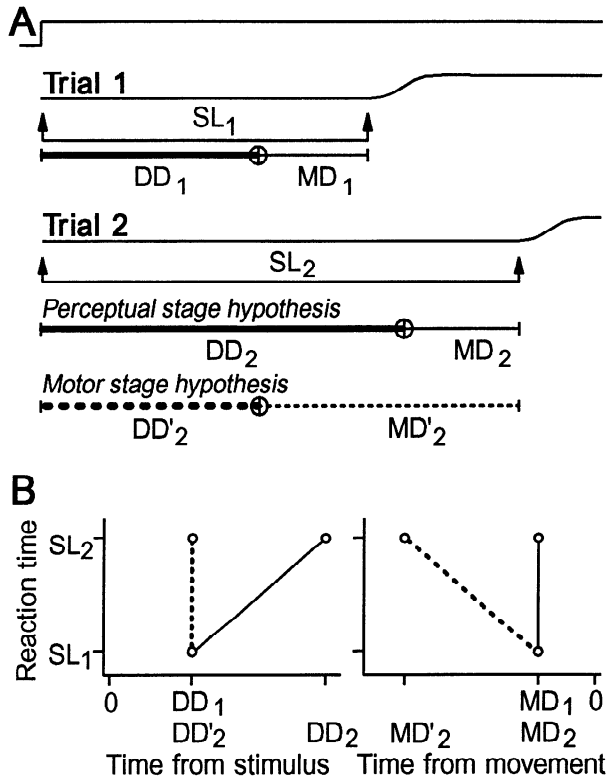

FIG. 1. Contrast of alternative hypotheses that the variability in reaction time originates in perceptual vs. motor processing stages. *A*: trial with a short reaction time is compared with a trial with a long reaction time. *Top trace*: time of stimulus presentation. Indicated directly under the eye position traces are the saccade latencies (SL). SL_1: shorter saccade latency. SL_2: longer saccade latency. Saccade latency is subdivided into 2 time intervals. The 1st interval is termed discrimination duration (DD) and represents the amount of time taken to discriminate the location of the saccade target. The 2nd interval is termed motor duration (MD) and represents the amount of time taken to initiate a saccade after target discrimination. These 2 time intervals are demarcated by the target discrimination time (TDT) (⦶). The increase in reaction time in Trial 2 over Trial 1 can be attributed to either an increase in DD (perceptual stage hypothesis) or an increase in MD (motor stage hypothesis). The perceptual stage hypothesis states that DD changes with saccade latency ($DD_2 > DD_1$) and MD does not change with saccade latency ($MD_2 = MD_1$); thus the time taken for saccade initiation is directly related to the time taken to discriminate the target. The motor stage hypothesis states that MD changes with saccade latency ($MD'_2 > MD_1$) and DD does not change with saccade latency ($DD'_2 = DD_1$); thus the time taken for saccade initiation is directly related to the time taken to generate a saccade after target discrimination. *B*: relationship of reaction time to DD and MD predicted by the discrimination and motor stage hypotheses. *Left*: saccade latency is plotted as a function of DD with the time of stimulus presentation at *time 0*. A line connecting the points predicted by the perceptual stage hypothesis (—— between DD_1,SL_1 and DD_2,SL_2) would have a slope of 1 because saccade latency is a direct function of the time taken for target discrimination. A line drawn between the points predicted by the motor stage hypothesis (- - - between DD_1,SL_1 and DD'_2,SL_2) would have an infinite slope because the time taken to discriminate the target does not change with saccade latency. *Right*: saccade latency is plotted as a function of MD with the time of saccade initiation at *time 0*. MDs are plotted as negative numbers indicating time before the saccade. A line connecting the points predicted by the perceptual stage hypothesis (—— between MD_1,SL_1 and MD_2,SL_2) would have an infinite slope because the time taken to generate a saccade after target discrimination does not change with saccade latency. A line drawn between the points predicted by the motor stage hypothesis (- - - between MD_1,SL_1 and MD'_2,SL_2) would have a slope of −1 because saccade latency is a direct function of the time taken to generate a saccade after target discrimination.

target discrimination by most FEF cells did not predict saccade latency, casting doubt on the perceptual stage hypothesis and lending support for the motor stage hypothesis. We propose, therefore, that during a popout visual search task the target discrimination process measured in FEF cells registers the outcome of perceptual processing, and the wide variability in saccade latencies arises during the processing necessary for response selection, preparation, and initiation.

Some of the findings presented in this report have appeared in abstract form (Thompson et al. 1995).

METHODS

Subjects and surgery

Data were collected from three *Macaca mulatta* weighing 4–10 kg. The animals were cared for in accordance with the National Institutes of Health Guide for the Care and Use of Laboratory Animals and the guidelines of the Vanderbilt Animal Care Committee. The surgical procedures have been described previously (Hanes et al. 1995; Schall 1991a; Schall et al. 1995a).

Behavioral training and tasks

Detailed descriptions of the behavioral training and tasks have appeared previously (Hanes et al. 1995; Schall et al. 1995a). With the use of operant conditioning with positive reinforcement, the monkeys were trained to perform a task in which a juice reward was contingent on accurately executing a saccade to a target presented alone or with distractors. Figure 2 illustrates the two primary task conditions. Stimuli were presented on a video monitor with a 60-Hz refresh rate. After fixation of a central spot for ~500 ms, a target appeared at a peripheral location. The location of the target varied in a pseudorandom sequence within a block of trials. To map the response field, the target was presented alone at 1 of 6, 8, or 12 positions varying in direction or eccentricity. In the search condition the target was presented at one of eight isoeccentric locations equally spaced around the central fixation spot along with distractors at the other seven locations. The targets and distractors were distinguished by either color (red vs. green) or form (high- vs. low-spatial-frequency square wave, high-contrast checkerboards). The target and distractors were switched between but not within blocks of trials. If monkeys are given exclusive experience with one target and set of distractors, then the initial visually evoked activity of many neurons in FEF discriminates the target (Bichot et al. 1996a). All of the data used in this study were from cells that did not discriminate the target from distractors in their initial visual activation.

Data collection and analysis

Standard techniques were used to collect these data (Hanes et al. 1995; Schall 1991a; Schall et al. 1995a). In two of the monkeys (*monkeys B* and *C*), electrodes were inserted through guide tubes positioned in a grid with holes spaced at 1-mm intervals (Crist et al. 1988). In the following we describe differences in analytical methods from those we have used previously, describe analyses relevant to this study of the time course of visual activation and target discrimination, and append descriptions of methods previously given (Hanes et al. 1995; Schall et al. 1995a).

Spike density functions

Spike density functions have traditionally been constructed by replacing each spike with a Gaussian function of a specific or variable SD (Chelazzi et al. 1993; Levick and Zacks 1970; Rich-

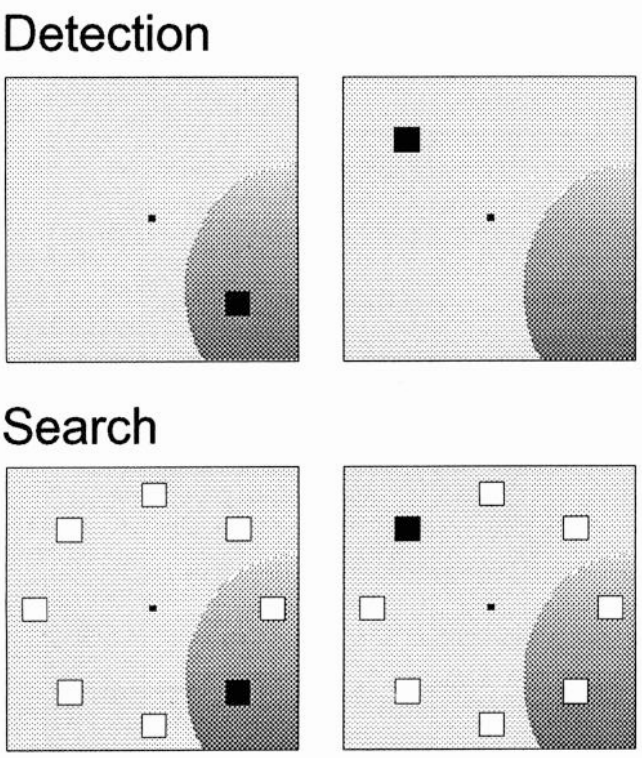

FIG. 2. Schematic representation of trial conditions. Each trial began with presentation of a white spot at the center of a video monitor. A change of color of the fixation spot (trigger signal) instructed the monkey to shift gaze to the target. The color change of the fixation spot occurred simultaneously with the presentation of the stimuli. In detection trials the target was presented alone. In search trials the target was presented with distractors. Each shaded region represents a cell's receptive field. The location of the target varied randomly, so that on any given trial the target could appear in the cell's receptive field (*left*) or outside the receptive field (*right*). In search trials, when the target appears outside the receptive field, distractors appear in the cell's receptive field.

mond and Optican 1987; Richmond et al. 1990; Schall et al. 1995a; Segraves and Park 1993; Waitzman et al. 1988). Use of a symmetric Gaussian filter is motivated by the assumption that the spike could have occurred at different times, with the probability represented by the width of the Gaussian. Although this is useful in some cases, for the questions we are proposing we decided that it is important to represent what the neuron actually did and not what could have happened. The Gaussian spike density function systematically underestimates times determined relative to stimulus presentation because of the apparent influence of spikes backward in time. Moreover, we know of no principled means of specifying the SD of the Gaussian filter. Therefore we created a new spike density function designed to represent the postsynaptic consequences of cell activity. With this goal in mind, the spike train was convolved with a combination of growth and decay exponential functions that resembled a postsynaptic potential given by the equation

$$R(t) = [1 - \exp(-t/\tau_g)] \cdot [\exp(-t/\tau_d)]$$

where rate as a function of time $[R(t)]$ varies according to τ_g, the time constant for the growth phase, and τ_d, the time constant for the decay phase. Physiological data from excitatory synapses indicate that 1 and 20 ms are good values for τ_g and τ_d, respectively (Kim and Connors 1993; Mason et al. 1991; Sayer et al. 1990; Thomson et al. 1993a,b). The spike density functions in this report are of this type.

This asymmetric spike density function has two advantages. First, each spike exerts influence only forward in time; this represents the actual postsynaptic influence of each cell. Second, because a function that resembles a postsynaptic potential was used, time constants that are comparable with actual physiologically measured values were used. Another motivation for the use of the postsynaptic potential filter for the time course analysis is that when we used the Gaussian filter, target discrimination times (TDTs) occasionally occurred earlier than the obvious visual latency of the neuron. This impossibility resulted because of the fact that with the Gaussian filter, spikes exert influence backward in time. To evaluate the performance of both filters, we analyzed a subset of the neurons included in this study ($n = 10$) with a spike density function derived from a Gaussian filter with a 4-ms SD. Estimates of TDTs ranged from 3 to 20 ms earlier and averaged 8.5 ms earlier than the times reported in this study. We believe the physiologically plausible filter provides more reliable information.

Poisson spike train analysis

Latencies of visual responses were determined with the use of a Poisson spike train analysis. The details of the analysis and application of this method to movement-related activity are described in Hanes et al. (1995). We have now developed this algorithm further to identify multiple periods of activation within single trials and to detect weak activation across trials. The performance of this method is illustrated in Fig. 3. This neuron was chosen for illustration because it had two periods of activity, neither of which was consistently observed on every trial. First, the Poisson spike train analysis was applied to each trial to identify periods of activity in which more spikes occurred than predicted from a Poisson random process having the overall average rate of the trial. For each

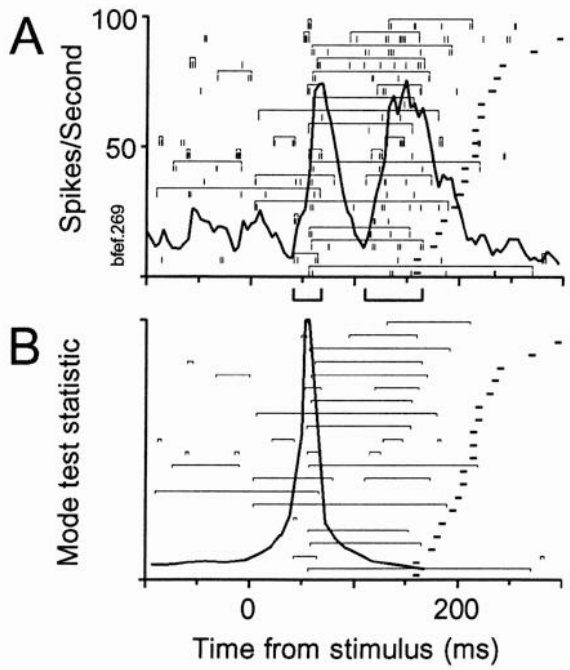

FIG. 3. Determination of visual response latency. *A*: raster display and spike density function of a visually responsive frontal eye field (FEF) neuron. Each line of rasters represents the activity on 1 trial; trials are sorted by saccade latency. Horizontal bars: time of saccade initiation. Brackets above each raster line: periods of significantly elevated activity identified by the Poisson spike train analysis. Brackets below abscissa: periods of significantly elevated activity as determined by the Poisson spike train analysis applied across all trials. *B*: periods of significantly elevated activity on single trials are replotted. The function plotted is the mode estimation of the beginning of activation of each period ($N = 44$, $J = 11$).

cell the mode of the distribution of response beginning times for all trials was estimated (*Eq. 13.3.1* in Press et al. 1988). First, the times of the beginnings of responses (t) across all trials were sorted into ascending order. Next, an integer J was selected as the window size over which the distribution function was smoothed. Reliable estimates of the mode resulted when J was set as 1/4 of the total number of periods of significant activations (N) but no less than 3. Next, for every $i = 1,..., N-J$ the mode test statistic (p) was estimated by the following equation

$$p[(t_i + t_{i+J})/2] = J/N(t_{i+J} - t_i)$$

The time of $(t_i + t_{i+J})/2$ that generates the largest value of p was the estimated mode, and represented the visual latency of the cell. Figure 3*B* plots this mode statistic as a function of time. The cell in Fig. 3 had two discrete phases of activation revealed by the spike density function. In some single trials the Poisson algorithm identified the two periods, but in other trials only a single period of activation was detected. The mode of the latencies of the earliest beginning of activation in each trial was 57 ms. For a minority of the cells analyzed, the activity was weak and the Poisson analysis generally failed on single trials. For these cells, the Poisson analysis algorithm was applied after collapsing spikes across all trials into one histogram with 1-ms bins. The spike counts for the Poisson analysis algorithm were derived from the histogram. The outcome of this alternate method is illustrated by the two brackets beneath the abscissa in Fig. 3*A*. The periods of significant discharge agrees with the modulation of the spike density function. Of the 84 cells analyzed, it was necessary to apply the Poisson analysis across trials for only 9 cells when the search target stimulus fell in the receptive field, for 15 cells when a search distractor stimulus fell in the receptive field, and for only 7 cells when the detection target fell in the receptive field.

Visual latency estimates were corrected for the raster scan time on the basis of the location of the receptive field on the video monitor. Corrections ranged from 2.5 to 13.7 ms and averaged 7.9 ms.

Analysis of the time course of target discrimination

We used a method adopted from signal detection theory (Green and Swets 1966) to determine when the activity evoked by the target of a search array can be distinguished from the activity evoked by the distractors. To do this, we compared the distribution of discharge rates during trials when the target fell in the response field (the response field often encompassed 2 or 3 of the possible target locations, see Fig. 2) with the distribution of discharge rates during trials when the target fell at up to three locations in the hemifield opposite the response field, and only distractors were in the response field. For example, if the response field encompassed the area indicated in Fig. 2, then the activity during trials when the target landed at the two locations inside the response field (right and down/right) would be compared with the activity during trials when the target landed at the left and up/left locations. We have previously reported that the activation evoked by distractors when the target is located next to the response field is suppressed more relative to when the target is distant from the response field in a fraction of cells (Schall and Hanes 1993; Schall et al. 1995a). For this analysis, the locations flanking the response field were not used, to avoid potential problems resulting from combining two different distributions of activity.

Of course, this comparison of the activity of a single neuron in two different behavioral conditions is not available to the brain in real time. The assumption made by this analysis is similar to the idea of an "antineuron" used by Britten et al. (1992). The comparison is essentially between the activation of the neuron under study and the activation of a hypothetical neuron that is identical except that it discharges in relation to saccades made in the opposite direction. Methods exist to analyze eight instead of two alternatives, but we believe the potential gains in rigor are not compensated for by greater insight into the phenomenon. It is important to note that this method is only a tool that is used to describe the discrimination process through time. Nevertheless, we suspect that this analysis reflects essential elements of an actual comparison that the brain performs on any given trial between the populations of neurons that have the target in their response fields and the population of neurons that have only distractors in their response fields.

Figure 4, which illustrates the method, shows a scatterplot of the discharge rates at 5-ms intervals from single trials when the target of the search array landed in the response field and when only distractors landed in the response field. Spike density functions on each individual trial were calculated to determine the discharge rates. Each symbol indicates the discharge rate for a single trial at the time indicated on the abscissa. The individual spike trains from which these distributions were obtained and the overall average spike density functions across all trials are shown in Fig. 7*A*. Because we wanted to relate the evolution of activity to saccade initiation, spikes occurring after saccade initiation on each trial were not included in the calculation of the spike density functions. The discharge rates determined for each 5-ms interval on each trial were averaged over 10 ms (from 5 ms before to 5 ms after) to smooth the data. This smoothing decreased the variability and facilitated the fitting of the resulting data points with a Weibull function (explained below). Intervals of 5 ms were used because it allowed for a sensitive estimate of the time course of changes; measurements over longer intervals compromised the resolution of the analysis.

At each time interval, the separation of the two distributions of activity obtained when the target or distractors fell in the response field was quantified by calculating receiver operating characteristic (ROC) curves (Egan 1975; Green and Swets 1966; Macmillan and Creelman 1991). This method has previously been used to analyze the ability of single neurons to discriminate stimulus features (Bradley et al. 1987; Britten et al. 1992; Guido et al. 1995; Tolhurst et al. 1983; Vogels and Orban 1990; Zohary et al. 1990). Example ROC curves are shown in Fig. 4. A point on an ROC curve is generated by plotting the probability that the activity when the target was in the response field was greater than a criterion as a function of the probability that the activity when distractors were in the response field was greater than that criterion. To generate the entire ROC curve the criterion level is incremented from zero to the maximum discharge rate obtained on a single trial. The value to increment the criterion level is not critical except that it needs to be small enough to generate an adequate number of points to generate an accurate ROC curve. For this study, criterion levels were set at 4-spike/s intervals. For cells that ultimately signal whether the target is in the response field, the ROC curves bow away from the diagonal with increasing time after search array presentation. The area under the ROC curve is a quantitative measure of the separation of the two distributions. The target discrimination process was quantified by plotting the area under the ROC curve as a function of time (Fig. 7*B*). Values of the area under the ROC curve increase from ~0.5 to ≤1.0. The area under the ROC curve could be interpreted as an estimate of the probability of an ideal observer correctly discriminating whether the target is in the response field. For our purposes it is sufficient that this method provides a reliable estimate of the separation of the neural activity into two distributions.

To describe the growth in the area under the ROC curve with time, the data were fit with a cumulative Weibull function

$$P = 1 - 0.5 \cdot \exp[-(t/\alpha)^{\beta}]$$

where t is time after stimulus presentation or before saccade initiation, α is the time at which the curve reaches 64% of its full growth

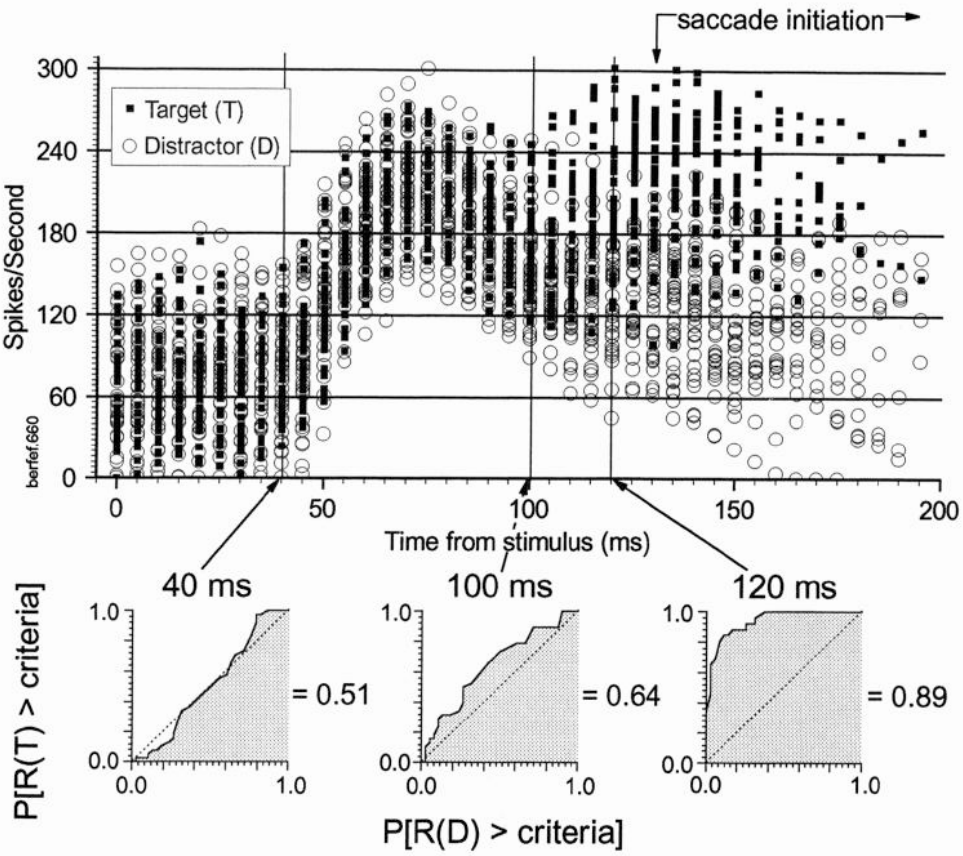

FIG. 4. Scatterplot of the discharge rate measured in 5-ms intervals derived from spike density functions as a function of time after presentation of the search array stimulus. Filled squares: activity when the target fell in the response field. Open circles: activity when only distractors fell in the response field. The interval during which saccades were made is indicated at the *top*. A receiver operating characteristic (ROC) analysis was used to quantify the separation of the target-evoked and distractor-evoked distributions of activity at each 5-ms step of time. The criterion levels used were at 4-spike/s steps (indicated on the ordinate). Representative ROC curves are shown for the distributions at 40, 100, and 120 ms (| in the scatterplot). The area under the ROC curve ranges from ~0.5 (indicating overlapping distributions) to 1.0 (indicating separate distributions). The area under each ROC curve is noted.

(this corresponds to an area under the ROC curve value of 0.82 when the curve begins at 0.5 and reaches 1.0), and β is the slope. Our preliminary analyses of the data indicated that the ROC area for many cells did not reach 1.0, nor did it necessarily have initial values of precisely 0.5. To account for this, we also fit the points with the function

$$P = \gamma - (\gamma - \delta) \cdot \exp\left[-(t/\alpha)^{\beta}\right]$$

where γ is the maximum value and δ was the minimum value of the curve. The quality of the fits was evaluated with the model selection criterion (Akaike 1976) as detailed in Schall et al. (1995a). The function yielding the best fit as determined by the model selection criterion statistic was used to estimate the time of target discrimination. The time of target discrimination was set as the time when the best fit function reached 0.75. For data best fit by the four-parameter function, if γ was <0.75, we judged that the cell did not discriminate the target. Because there was a wide range of saccade latencies, the time of target discrimination may not be accurately measured if this analysis was performed only when trials were aligned on stimulus presentation. To verify the accuracy of the measurement, the time of target discrimination (see Fig. 1) was also determined with the trials aligned on saccade initiation. In this case, the time of target discrimination was set as the time when the best fit function first reached 0.75 going backward in time from the time of saccade initiation. In this report the term TDT indicates the instant when the best fit function reaches 0.75. The term discrimination duration (DD) indicates the length of time from stimulus presentation to TDT, and the term motor duration (MD) indicates the length of time from TDT to saccade initiation. Subscripts are used where needed to specify whether DD or MD was calculated from trials aligned on stimulus presentation (DD_{stim}, MD_{stim}) or aligned on movement initiation (DD_{move}, MD_{move}). DD_{stim} and MD_{move} are the most accurate estimates because they are anchored by the aligning events. The accuracy of the estimate of TDT was checked by comparing the sum of DD_{stim} and MD_{move} with the mean saccade latency of the group of trials being analyzed. The same results are obtained if one uses the median saccade latency.

For some cells it was necessary to limit the range of times for the curve fits. Occasionally excessive variability in ROC areas occurring before the visual response latency and after saccade initiation made it impossible to fit the data to the cumulative Weibull curve across the entire span from stimulus presentation to saccade initiation. In those cases, the Weibull curve was fit over the span of time representing the evolution of activity from nondiscriminating to the completion of discrimination for that cell. Overall, the best fit Weibull curves accurately represented the change in ROC area with time as judged by the r^2 values obtained from each cell (mean $r^2 = 0.85$, range 0.32–0.99).

To determine whether the time taken for target discrimination accounted for variations in reaction time, we partitioned the data from individual cells into three groups on the basis of saccade latency. To provide a uniform basis for comparison, lower and upper saccade latency tail limits were empirically determined. In this report the lower latency limit was 130 ms and the upper limit was 300 ms. Trials with saccade latencies outside the lower and upper limits were eliminated; only 1% of the trials were removed. The remaining trials were divided into the early, middle, and late thirds of the saccade latency distribution. The monkey's performance could change from day to day and also could change during a recording session as the monkey fatigued. For this reason the ranges of saccade latencies within each group were determined separately for each cell recorded. The minimum number of trials needed for the ROC analysis depended on the magnitude and relia-

bility of discharge on single trials for each cell. For a few cells, as few as four target or distractor trials were sufficient. For nearly all of the saccade latency groups there were ≥10 target and 10 distractor trials, which provided ample data for the ROC analysis. To provide an unconfounded basis for comparison of the neural activity, a nonparametric Watson's U^2 test (chapter 4 of Batschelet 1981) was performed on the distributions of saccade latencies to make sure that the latencies when the target was in the response field did not differ from the latencies when a distractor was in the response field.

Relating times of modulation to behavioral events

Statistical tests were performed to determine whether DD and MD were related to stimulus presentation or to saccade initiation (Commenges and Seal 1985, 1986). The key statistic was the ratio of the variances of the time of neural modulation relative to two possible events, e.g., target presentation or saccade initiation. If the ratio was significantly different from 1.0, on the basis of the F distribution, then the time of neural modulation was likely associated with the event with the least temporal variance.

Histological processing and track localization

Conventional histological procedures were used (Schall et al. 1995b). After perfusion, the brains were removed, photographed, and blocked. *Monkey Q* was included in a previous tract tracing study (Parthasarathy et al. 1992) in which frontal cortex was sectioned coronally. We examined a series of Nissl-stained sections from this study. Before perfusion of *monkey B,* a set of fiducial pins were placed though the electrode placement grid. The frontal cortex of *monkey B* was blocked and sectioned approximately parasagitally in the plane of the electrode penetrations. Sections 40 μm thick were stained for Nissl (thionin). The paths of multiple electrode penetrations made through individual guide tube locations were evident from gliosis. Our analysis of the cytoarchitecture and myeloarchitecture of frontal cortex was guided by established descriptions (von Bonin and Bailey 1947; Walker 1940) supplemented by newer findings (Preuss and Goldman-Rakic 1991; Schall et al. 1995b; Stanton et al. 1989). The rostral bank and convexity of the arcuate sulcus can be subdivided into at least four areas. The region in the rostral bank of the arcuate sulcus containing concentrated large pyramidal cells in layer 5 has been identified as corresponding to the functionally defined FEF (Bruce et al. 1985; Stanton et al. 1989). The ventrolateral portion of this zone has been further distinguished by the presence of large pyramidal cells in layer 3 as well as layer 5 (Walker 1940). The ventrolateral zone is area 45, and the dorsomedial zone is area 8A. Area 8A can be subdivided. The cortex within the medial portion of the rostral bank of the arcuate sulcus contains few if any large pyramidal cells in layer 3 and a thin granular layer, and is referred to as area 8Ac. The transitional zone that forms the rostral boundary of area 8Ac and area 45 and adjoins the caudal boundary of area 46 is referred to as area 8Ar. In Nissl, area 8Ar has few large pyramidal cells and a more clearly defined layer 4 compared with 8Ac. In myelin, area 8Ar is characterized by conspicuous bands of Baillarger and radial fibers. The area we designate as 8Ac corresponds to areas 8Ac and 8Am of Preuss and Goldman-Rakic (1991).

RESULTS

The first aim of this study was to determine whether the visual response latency of FEF neurons differed when the target for a saccade was presented alone or with distractors or when only distractors fell in the cells' receptive fields. The second aim was to test the hypothesis that delays in the time of target discrimination accounted for delays in the latencies of saccades to the target. A total of 291 cells was collected from three monkeys. Of those cells, 84 exhibited activity related to the presentation of the stimulus and provided sufficient data in the necessary trial conditions to be included in this report. Of these cells, 51 were from *monkeys B* and *Q* and have been included in previous reports on the target selection process within macaque FEF (Schall and Hanes 1993; Schall et al. 1995a). For this report, *monkey C* contributed an additional 33 cells.

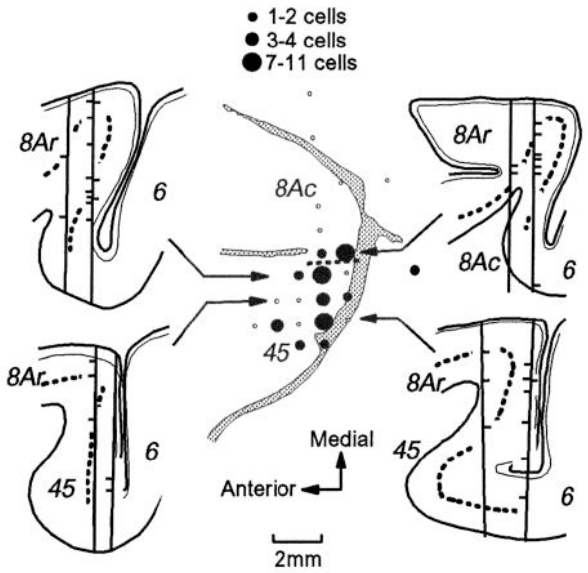

FIG. 5. Location of cells in *monkey B.* The entry points of electrode penetrations in which visual and/or saccade related activity was recorded are shown on a rendering of the arcuate cortex. Open circles: locations where electrode penetrations were made. Filled circles: penetrations in which neurons analyzed for this study were encountered. Size of the filled circle indicates the number of neurons according to the legend. Horizontal dashed line: midpoint of the transition between areas 8Ac and 45. Representative coronal sections from the indicated levels show the paths of penetrations made with the use of the guide tube grid. Tick marks: approximate depth at which the cells were recorded. Cytoarchitectonic areas are indicated. Dashed line in each section: layer 4.

The electrode penetrations have been histologically localized to FEF in the rostral bank of the arcuate sulcus in *monkeys Q* and *B* (Fig. 5). Figure 1 of Schall (1991b) shows the entry points of electrode penetrations in *monkey Q* that encountered task-related cells in the arcuate cortex. We have subsequently examined the cortex of *monkey Q* histologically to confirm that the penetrations were made in the rostral bank of the arcuate sulcus. Figure 5 shows the histological analysis of *monkey B.* The cells contributing to this investigation were recorded in the rostral bank of the arcuate sulcus. Most of the cells were in area 45 and lateral area 8Ac, with a few cells found in caudal area 8Ar. Physiological recordings are continuing in *monkey C,* but the electrode penetrations in this animal advanced through the rostral bank of the arcuate sulcus as identified by the sulcal pattern observed at the time of the craniotomy and the incidence of visual and saccade-related activity. FEF location was also confirmed by the depths of the cells and the ability to evoke saccades with low-threshold electrical microstimulation. There were no significant differences in the results from the

three monkeys, nor were there significant differences in the results with search arrays defined by color or by form. Therefore all cells will be considered together.

For this investigation neurons were analyzed that responded in relation to the presentation of visual stimuli presented at eccentricities ranging from 4 to 20°. Visual responses were identified by their constant latency relative to the time of stimulus appearance. With the single-target task, by imposing an instructed delay between the appearance of the target and the trigger signal to make the saccade, it was possible to subdivide these visually related neurons. Some neurons had a single phasic response to the visual stimulus ($n = 12$) (see Fig. 8). Most exhibited more tonic responses, discharging from target presentation through the saccade, and often had increasing activity before a saccade into their response field ($n = 72$) (see Fig. 7*A*). We refer to this latter group as visuomovement cells. Unfortunately, a memory-guided saccade task to a flashed target, which would have allowed us to definitively distinguish visuomovement cells from tonic visual cells (Bruce and Goldberg 1985), was rarely used. The absence of this test, however, does not compromise the interpretability of the results we report. Moreover, those cells that could be reliably classified as tonic visual or visuomovement did not differ in the measures reported in this study.

Visual response latency

The visual latency was determined separately for trials when the search target, search distractors, and detection target were presented in each cell's receptive field. The cumulative distributions of these FEF visual latencies are shown in Fig. 6. The latency values across the population of FEF cells obtained from all three conditions did not differ [analysis of variance (ANOVA), $F(2,237) = 1.66$] even though the magnitude of the visual responses to the search display were attenuated compared with the visual responses to the target presented alone (Schall et al. 1995a). The average latency across all cells was 67 ± 3 (SE) ms for the search target, 67 ± 2 ms for the search distractor, and 67 ± 3 ms for the detection target. Because the visual response latencies obtained with the three stimulus conditions did not differ significantly, the values were averaged to assign a visual response latency to each FEF neuron. A frequency distribution of the visual response latencies of FEF cells is shown in Fig. 12*A*. Overall, the visual response latencies for this sample of FEF neurons ranged from 35 to 138 ms and averaged 67 ± 2 ms. The mean and range of visual response latencies we measured in FEF are comparable with those reported previously (Bruce and Goldberg 1985; Goldberg and Bushnell 1981; Schall 1991b).

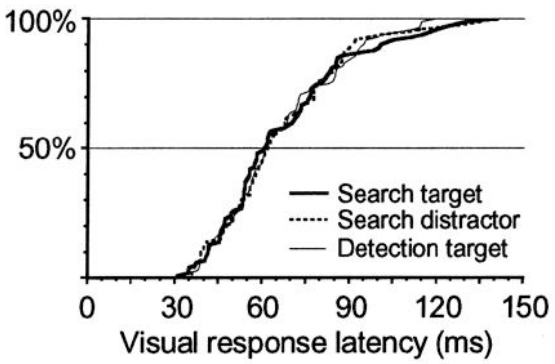

FIG. 6. FEF visual response latency. Cumulative distributions of the latencies of visual responses to the target in the response field during detection (thin ——), to the target presented in the response field during visual search (thick ——), and to only distractors in the response field during visual search (- - -).

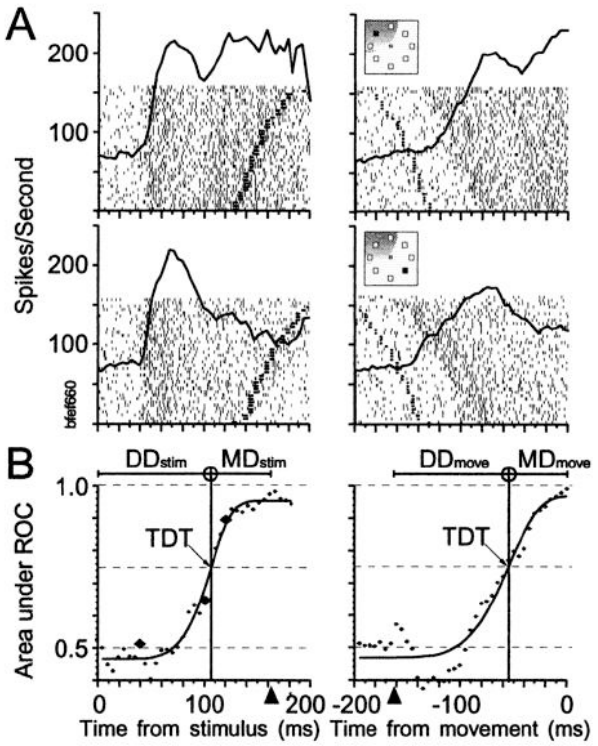

FIG. 7. Time course of target discrimination of the FEF visuomovement cell illustrated in Fig. 4. *A*: raster plots of the response to a search display aligned on stimulus presentation, at time 0 (*left*) and on saccade initiation at time 0 (*right*). Each line of rasters represents the activity on 1 trial; trials are sorted by saccade latency. The average spike density across all trials is also plotted in each of the raster plots. Horizontal bars: time of saccade initiation (*left*) and time of stimulus presentation (*right*). *Top*: activity in trials in which the target was presented in the cell's receptive field. *Bottom*: activity in trials in which only distractors were presented in the cell's receptive field. The receptive field location for this cell is illustrated as the shaded region in visual display *insets*. *B*: area under the ROC curve derived from the activity shown in *A* is plotted as a function of time aligned on stimulus presentation (*left*) and aligned on saccade initiation (*right*). The large filled diamonds on *left* highlight the values from the ROC curves shown in Fig. 4. Solid lines: best fit Weibull functions. Horizontal dashed lines: levels of ROC area of 0.5, 0.75, and 1.0. The time at which the function reached a threshold value of 0.75 is indicated by the vertical line intersecting the Weibull function and the horizontal line at 0.75. Triangle below the abscissa: mean saccade latency (*left*) and mean stimulus presentation time (*right*). Above the plots the mean saccade latency is divided into DD and MD. Subscripts indicate whether the trials were aligned on stimulus presentation or movement initiation. TDT is indicated by the encircled vertical bar. Although the trials were aligned differently, $DD_{stim} \approx DD_{move}$ and $MD_{stim} \approx MD_{move}$.

TDT

Figure 7*A* shows the activity from a representative FEF neuron recorded while a monkey was performing the popout visual search task. The distributions of activity during single

trials aligned on stimulus presentation were shown in Fig. 4. This cell began discharging on average 42 ms after stimulus presentation. By comparing the trials in which the target landed in the response field with trials in which only distractors landed in the response field, one can see that at some point in time after the initial visual response, the activity of this cell discriminated whether the target or a distractor was in the receptive field. If the target was in the cell's receptive field, the discharge rate remained elevated. If only distractors were in the cell's receptive field, the activity became somewhat suppressed even though the image was still on the retina and the eyes had not yet moved.

The instant in time when the activity of FEF neurons discriminated whether the target or only distractors were in the response field was determined with the use of an ROC analysis that quantifies the separation of the distributions of the neural activity in the two stimulus conditions. Figure 7*B* plots the area under the ROC curve as a function of time. Just as the raster displays can be aligned on either the time of stimulus presentation or the time of saccade initiation, so also can the plots of ROC area be aligned on either of the two events. The area under the ROC curves increased with time from search array presentation, indicating that the cell's activity evolved to discriminate the target from distractors and that the reliability of this discrimination increased with time. To estimate the time course of this visual discrimination process, we fit the plot of ROC area as a function of time with a Weibull function. The time to reach a designated threshold provides an estimate of the latency of the discrimination process. We elected to establish an absolute threshold level for the area under the ROC curves to reach to be considered a decision by that cell because the area under the ROC curve is a quantitative measure of the separation between two distributions. We defined the TDT as the instant when the best fit Weibull function reached 0.75. This threshold value was chosen because it is the midpoint between chance and perfect discrimination. The length of time from stimulus presentation to TDT was termed DD, and the length of time from TDT to saccade initiation was termed MD. To verify the accuracy of our measurement method, a TDT was determined twice for each cell, once relative to stimulus presentation and again relative to saccade initiation. Subscripts indicate whether the calculation was performed with trials aligned on stimulus presentation (DD_{stim}, MD_{stim}) or aligned on movement initiation (DD_{move}, MD_{move}). Because these intervals are anchored by the aligned event, DD_{stim} and MD_{move} are more reliable estimates than are DD_{move} and MD_{stim}. But in nearly all cases $DD_{stim} \approx DD_{move}$ and $MD_{stim} \approx MD_{move}$.

The proportions of phasic visual cells and visuomovement cells that discriminated the target are listed in Table 1, as are the average values of DD_{stim}, MD_{move}, and saccade latency. Not all cells with a visual response discriminated the target of the search array. An example of a phasic visual cell that did not discriminate the target from distractors is shown in Fig. 8. A higher percentage of visuomovement cells than phasic visual cells discriminated the target of the search array. This is not surprising because phasic cells were not active long enough to reflect the discrimination process. For those cells that had activity that reached the 0.75 criterion, DD_{stim} averaged 141 ± 3 ms and MD_{move} averaged 53 ± 4 ms. Neither DD_{stim} nor MD_{move} differed significantly across the three monkeys [ANOVA, $F(2,55) = 0.80$].

Relation of reaction time to TDT

To determine whether the variation of reaction time could be accounted for by variation in DD or by variation in MD (as indicated in Fig. 1), the ROC analysis was performed on the activity of each cell after separation of trials into early, middle, and late saccade latency groups. An FEF cell illustrating the typical results is shown in Fig. 9. For this cell, DD did not increase as the saccade latency of the trials increased. However, from the short to the long saccade latency group, MD did increase. This result is evident in the plots aligned both on stimulus presentation (Fig. 9*A*) and on saccade initiation (Fig. 9*B*). In fact, the trials with the longest saccade latencies produced the shortest DD of the three groups. Validating the accuracy of our measurement, for all three saccade latency groups, the estimates of DD_{stim} and MD_{stim} (Fig. 9*A*) were nearly identical to DD_{move} and MD_{move} (Fig. 9*B*). This cell illustrates the overall trend we observed that the variation in DD did not account for the variation in saccade latency, whereas the variation in MD did account for the variation in saccade latency for a majority of the cells analyzed. This result casts doubt on the perceptual stage hypothesis and supports the motor stage hypothesis.

A crucial test of the accuracy of this ROC analysis is whether the TDTs estimated for the groups of trials with different saccade latencies are the same points in time if the calculations are performed on trials aligned on stimulus presentation or on saccade initiation. To test this for each group of trials from each cell, the values of DD_{stim} and MD_{move} were summed. If this sum was significantly different than the mean saccade latency, then we would conclude that the analysis is flawed because the alignment of the trials affects the estimate of TDT. A paired *t*-test comparing this sum for each group of trials with the mean saccade latency of the corresponding group of trials revealed no significant difference ($t_{260} = 0.91$). Thus the ROC analysis performed on trials aligned on stimulus presentation and on trials aligned on saccade initiation identified TDT as the same instant in time.

An *F* test was used to compare the variances of DD_{stim} and MD_{move} to determine whether at the population level TDT was more synchronized with stimulus presentation or with saccade initiation (Commenges and Seal 1985, 1986). The result of this test was that the variance of MD_{move} was significantly greater than the variance of DD_{stim} [$F(140,149) = 1.77$, $P < 0.001$], confirming that TDT was more related to the time of presentation of the search array than to the time of saccade initiation.

The previous analysis was based on population data. We also examined changes in saccade latency as a function of TDT for single cells as illustrated in Fig. 10. The plots in Fig. 10, *A* and *B*, are the basis for evaluating the alternative hypotheses as indicated in Fig. 1. The line segments in Fig. 10*A* were made for each cell by connecting the points representing the mean of the saccade latencies in each of the three groups of trials as a function of the DD_{stim} obtained from the activity in those trials. Figure 10*B* is the corresponding

TABLE 1. *Target discrimination: percentages of cells and processing stage durations*

	Percent Reaching 0.75 Criterion				Time, ms			
	Aligned on stimulus		Aligned on saccade					
	Phasic	Visuomovement	Phasic	Visuomovement	DD_{stim}	MD_{move}	DD_{stim} + MD_{move}	SL
All trials	17	78	8	68	140	53	193	192
Short SL	27	63	18	64	128	38	166	166
Middle SL	18	80	18	73	131	56	187	187
Long SL	18	81	9	74	146	77	223	222

Percentages of cells discriminating the target and the mean discrimination duration (DD) obtained by analyzing trials aligned on stimulus presentation (DD_{stim}), the mean motor duration (MD) obtained by analyzing trials aligned on saccade initiation (MD_{move}), and the mean saccade latency (SL) for the different saccade latency groups analyzed. The values obtained for all trials, short SL, middle SL, and long SL are listed separately in each row. *Left four columns:* percentages of the phasic visual and visuomovement frontal eye field (FEF) cells that discriminated the target in their response field [the area under the receiver operating characteristic (ROC) curve reached 0.75] when activity was aligned on stimulus presentation and when activity was aligned on saccade initiation. *Right four columns:* DD_{stim}, mean MD_{move}, mean sum of DD_{stim} and MD_{move}, and mean SL. For every group of trials, the values of DD_{stim} + MD_{move} and SL are nearly identical.

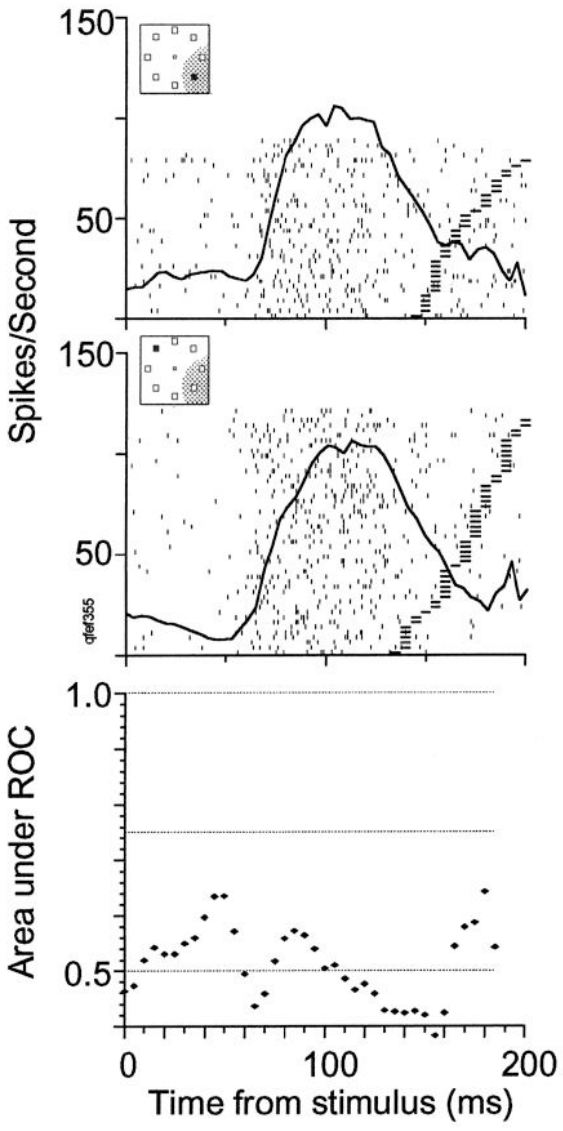

FIG. 8. Example of an FEF phasic visual cell that did not discriminate the target from distractors in its receptive field. Conventions as in Fig. 7. The area under the ROC never reached 0.75.

plot of mean saccade latency as a function of MD_{move} for the three saccade latency groups. If activity representing target discrimination reached the 0.75 criterion in all three saccade latency groups from a cell, then two line segments were drawn, one between the points from the short and the middle saccade latency groups and one between the points from the middle and long saccade latency groups. If the activity representing target discrimination reached the 0.75 criterion in only two saccade latency groups for a cell, then only one line segment between these two points was drawn. Cells with target- and distractor-evoked activity that produced ROC curves with areas that reached the 0.75 criterion in only one saccade latency group were left out of this analysis. Table 2 shows the number of cells having discriminative activity that reached the 0.75 criterion in different numbers of saccade latency groups for trials aligned on both stimulus presentation and on saccade initiation. A total of 49 cells with trials aligned on saccade initiation and 54 cells with trials aligned on stimulus presentation had at least two saccade latency groups in which the discriminative activity reached the 0.75 criterion. Because the monkey's performance changed from day to day and within each session, the ranges of saccade latencies associated with each cell making up the short, middle, and long saccade latency groups were not the same. Nevertheless, it is evident that most of line segments in Fig. 10 are inconsistent with the perceptual stage hypothesis and support the motor stage hypothesis.

The histograms in Fig. 10, *C* and *D,* show the distributions of the slopes of the line segments in Fig. 10, *A* and *B,* respectively. The slopes representing each cell were converted to degrees from the abscissa for ease of analysis. When all three saccade latency groups from a cell had discriminative activity that reached the 0.75 criterion, the two lines between the three points were averaged so that each cell contributed only one value in each distribution. As outlined in Fig. 1, if the time of target discrimination of FEF cells predicts saccade latency (according to the perceptual stage hypothesis), then the slope of the lines connecting DD values would be 1.0 (or 45° from the abscissa) and the slope of the line connecting MD values would be infinity (90°). Conversely, if the time of target discrimination does not vary with saccade latency (according to the motor stage

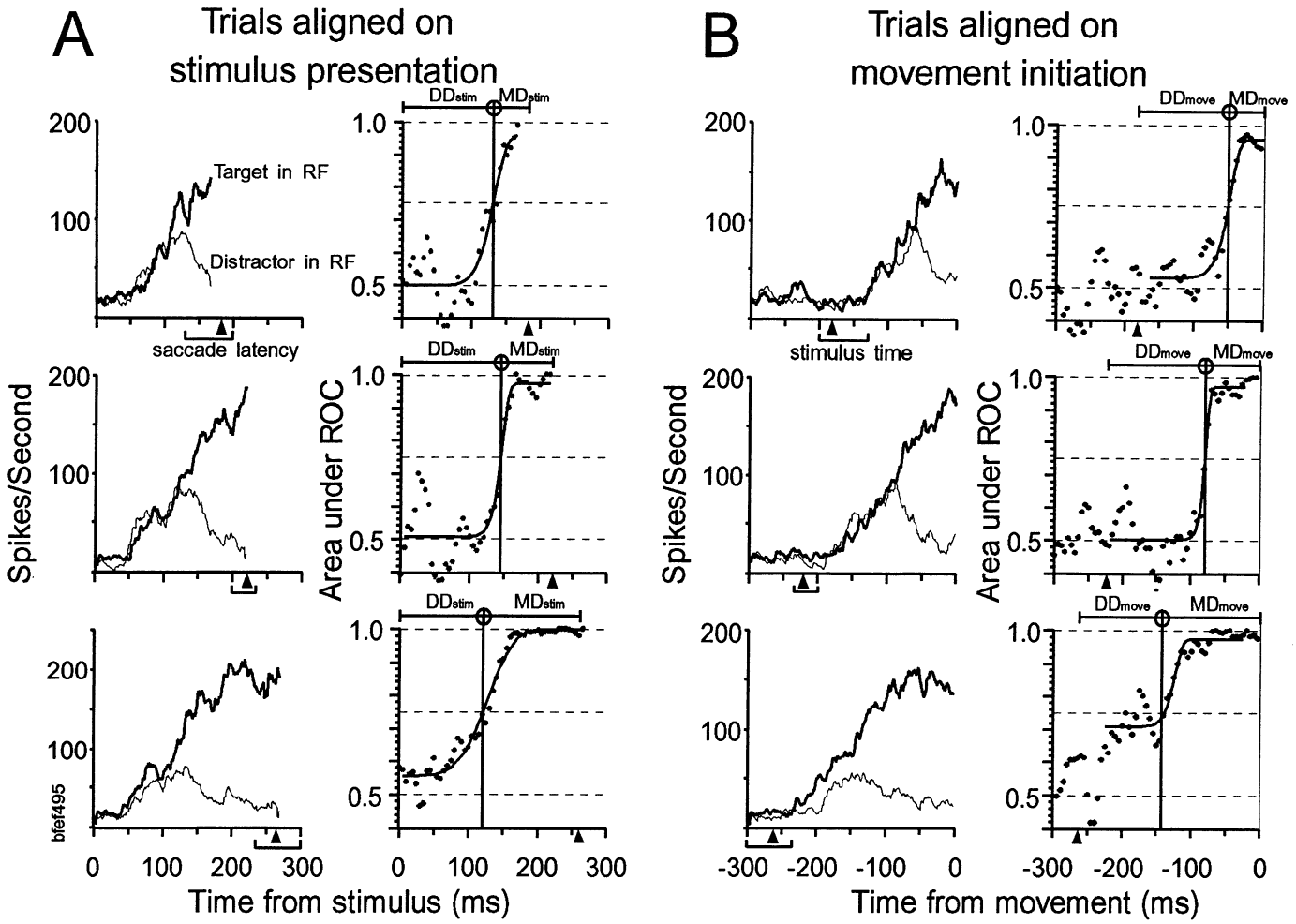

FIG. 9. Time course of target discrimination of an FEF visuomovement cell after trials were separated into short (*top*), middle (*middle*), and long (*bottom*) saccade latency groups. Plots are aligned on search array stimulus presentation in *A* and on saccade initiation in *B*. *A, left* and *B, left* plot the average spike densities when the target fell in the cell's receptive field (thick line) and when only distractors fell in the cell's receptive field (thin line). *A, right* and *B, right* plot the areas under the ROC curves at 5-ms intervals with the best fit Weibull functions. Circled vertical line: time the area under the ROC reached the 0.75 level (TDT). This time separates the mean saccade latency into 2 time intervals, DD and MD, illustrated above each Weibull function. In the spike density plots, the brackets beneath the abscissa indicate the range of saccade latencies comprising that group, and in all the plots the triangle below the abscissa indicates the mean saccade latency of that group. This cell discriminated the target at a time synchronized with stimulus presentation.

hypothesis), then the slope of the lines connecting DD values would be infinity (90°) and the slope of the lines connecting MD values would be −1.0 (135°). A *V* test was performed (Batschelet 1981) on the angular data to determine whether the observed angles cluster around the predicted angles. High *u* values result if the observed angles deviate significantly from randomness and are clustered around the predicted angle. The angles of the line segments derived from DD_{stim} values were not clustered around 45° [$V(45°)_{53}$, $u = 0.63$] but were significantly clustered around 90° [$V(90°)_{53}$, $u = 7.4$, $P < 0.001$]. The angles of the line segments derived from MD_{move} values were not clustered around 90° [$V(90°)_{48}$, $u = 0.82$] but were significantly clustered around 135° [$V(135°)_{48}$, $u = 7.2$, $P < 0.001$]. Thus, for the trials aligned on either the time of stimulus presentation or saccade initiation, the results show that the relation between TDT and saccade latency most closely follows the motor stage hypothesis, i.e., most of the variability of saccade latency arises from MD and not from DD.

Figure 10 indicates a clear diversity of results. Although for most cells the time of target discrimination was more correlated with the time of stimulus presentation, for some cells TDT was better synchronized with the time of saccade initiation. To obtain an overall estimate of what percentage of cells had TDTs that predicted saccade initiation and what percentage of the cells did not, the angles of the line segments in Fig. 10, *A* and *B*, were summed for individual cells. This was done so that TDTs obtained with trials aligned on stimulus presentation and with trials aligned on saccade initiation could contribute to this estimate. Summed angles of 135 or 225° would correspond to TDTs perfectly correlated with saccade initiation or stimulus presentation, respectively. Those cells with summed angles >180° were considered to discriminate the target location at a time relative to stimulus presentation; 78% (45 of 58) of the cells fell into this group. Those cells with angles <180° were considered to discriminate the target location at a time relative to saccade initiation; 22% (13 of 58) of the cells fell into this group.

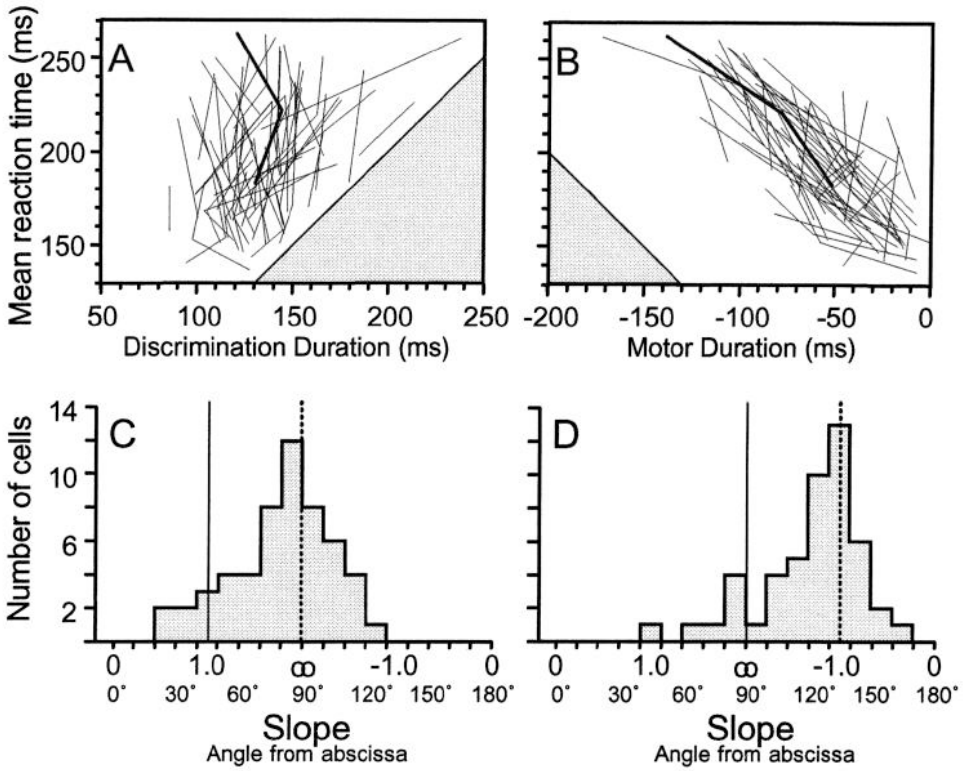

FIG. 10. Relationship of reaction time to the time of target discrimination for single FEF cells. *A* and *C*: comparison of DD_{stim} and saccade latency. *B* and *D*: comparison of MD_{move} and saccade latency. The 2 or 3 points on each line in *A* represent the mean saccade latency as a function of DD_{stim} for each saccade latency group in which the neural activity discriminated the target from the distractors to at least the 0.75 level. The points on each line in *B* represent the mean saccade latency as a function of MD_{move} for each saccade latency group in which the neural activity discriminated the target from the distractors to at least the 0.75 level. Some cells contributed 3 data points and others contributed just 2. Shaded region in *A*: time after saccade initiation. Shaded region in *B*: time before stimulus presentation. The thicker line segments in *A* and *B* are from the cell shown in Fig. 9. *C* and *D*: distributions of the average slopes of the line segments obtained for each cell in *A* and *B*, respectively. The slopes were converted to angles from the abscissa for ease of analysis. Solid vertical lines in *C* and *D* are located at the slopes of the line segments where TDTs occur at a consistent interval preceding saccade initiation, favoring the perceptual stage hypothesis in Fig. 1. Dashed vertical lines in *C* and *D* are located at the slopes of the line segments where TDTs occur at a consistent interval after stimulus presentation, favoring the motor stage hypothesis in Fig. 1.

For cells with activity that discriminated the target of the search array at a time more correlated with the time of stimulus presentation, DD_{stim} averaged 136 ± 3 ms (range 103–194 ms). For cells with activity that discriminated the target at a time more correlated with the time of saccade initiation, MD_{move} averaged 37 ± 6 ms (range 15–84 ms).

Time course of saccade target discrimination

The areas under the ROC curves provided an index of the quality of the discrimination as a function of time.

TABLE 2. *Number of cells discriminating the target in 0, 1, 2, or 3 saccade latency groups*

	0	1	2	3	Total
Aligned on stimulus	15	15	27	27	84
Aligned on saccade	18	17	23	26	84

Number of cells discriminating whether the target was present in their response field in 0, 1, 2, or all 3 saccade latency groups. *Top row*: number of cells with activity that discriminated the target when trials were aligned on stimulus presentation. *Bottom row*: number of cells with activity that discriminated the target when trials were aligned on saccade initiation.

The best fit Weibull functions were used to characterize the time course of the transition from the nondiscriminating state to discriminating whether the target was present in the response field. One possible measure was the parameter β, because it characterizes the slope of the Weibull function. However, the parameter β is unitless and thus does not indicate the rate of change of ROC area with time. Instead, to characterize the evolution of the target location signal, the beginning and end of the transition were estimated. Reliable estimates of these times were found to be the instants when the acceleration and deceleration of the Weibull function reached their respective peak values. This is illustrated in Fig. 11. The estimation of the beginning and end of this transition was performed only on those saccade latency groups with neural activity that yielded Weibull functions that accurately depicted the change in area under the ROC curve with time as judged by all the authors. The time at which the Weibull function crossed the 0.75 threshold was quite robust, but the estimates of the beginning and end of the transition from the best fit Weibull function were occasionally less certain. This is illustrated in Fig. 9*B, bottom right.*

From the times of the beginning and end of the transition

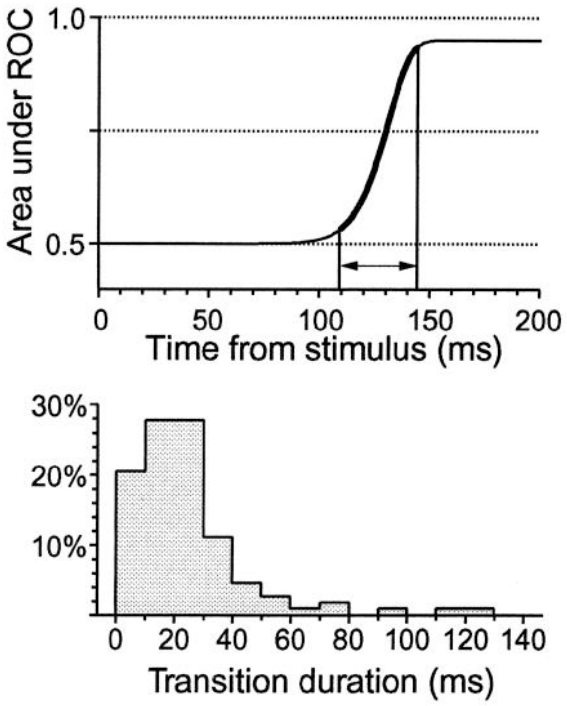

FIG. 11. Duration of the target discrimination transition. *Top*: typical Weibull curve that best fit the change in area under the ROC curve as a function of time. The thickened region of the Weibull function indicates the duration of the transition from the nondiscriminating state to discriminating whether the target is present in the response field; this interval of time is termed transition duration. *Bottom*: distribution of transition durations obtained for each group of trials in which the neural activity yielded a best fit Weibull function that reached that reached the 0.75 criterion and accurately reflected the beginning and end of the transition. Each cell could contribute up to 3 values, 1 for each saccade latency group. The transition duration was 25 ± 2 (SE) ms.

estimated from the best fit Weibull function, we were able to determine the rate of change of ROC area as a function of time. The linear slope between the beginning and end of the transition is termed the transition slope, and the duration of the transition is termed transition duration. An ANOVA was performed on the transition duration and on the transition slope between the short, middle, and long saccade latency groups. Neither the transition duration [ANOVA, $F(2,105) = 2.54$] nor the transition slope [ANOVA, $F(2,105) = 0.55$] differed significantly between groups of trials with differing saccade latencies. The transition slope averaged 0.017 ± 0.001 ms^{-1} and the transition duration averaged 25 ± 2 ms. The distribution of transition durations obtained from all saccade latency groups is plotted in Fig. 11, *bottom*. The discrimination process generally took between 10 and 30 ms to complete.

Figure 12 shows the temporal distributions of key neural events measured in the activity of FEF cells that lead to the generation of accurate saccades. Figure 12*A* shows the distribution of visual response latencies of all FEF cells analyzed ($n = 84$). The distributions in Fig. 12, *B–D*, illustrate the times of the beginning, middle, and end of the transition from the nondiscriminating state to the discriminating state. These data are from the groups of trials with activity that produced ROC curves with areas that reached the 0.75 level and were judged to accurately represent the discrimination process. Also shown in Fig. 12*C* is the distribution of TDTs obtained from all three saccade latency groups aligned on stimulus presentation. The saccade latency distribution of >6,000 visual search trials is shown in Fig. 12*E*. The variances of the times of beginning, middle, and end of the transition were all significantly smaller measured relative to stimulus presentation than measured relative to saccade initiation [beginning of transition: $F(107,107) = 1.88$, $P < 0.001$; middle of transition: $F(107,107) = 1.67$, $P = 0.004$; end of transition: $F(107,107) = 1.51$, $P = 0.016$]. The responses to the target versus the distractors in the receptive field begins to discriminate on average 117 ± 2 ms after stimulus presentation. Over time the reliability of the discrimination grew as indexed by the area of the ROC. This transition reaches its midway point 130 ± 2 ms after stimulus

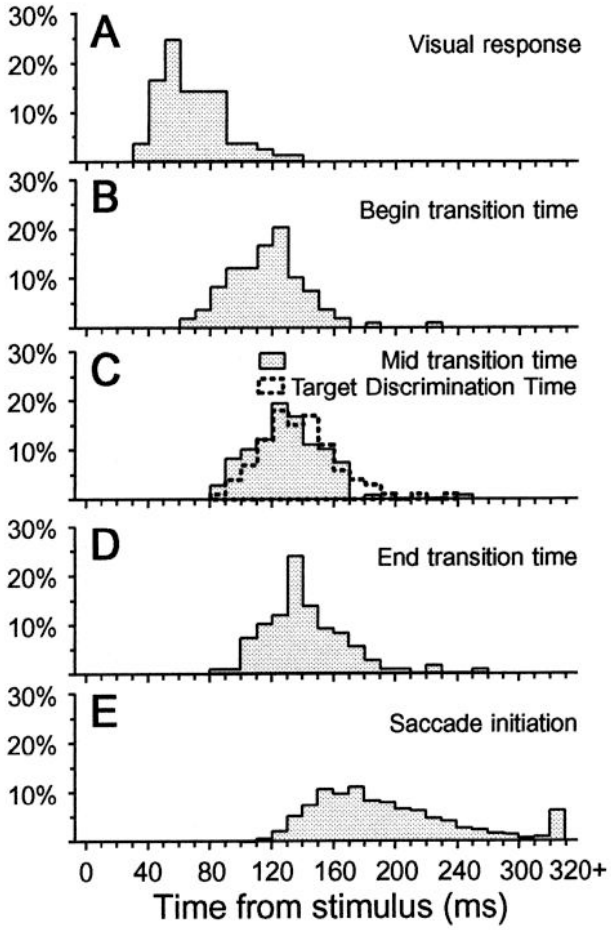

FIG. 12. Temporal distributions of key neural events related to target discrimination in the FEF before saccade initiation. *A*: distribution of visual response latencies of FEF cells ($n = 84$). *B*: distribution of the beginning of the transition obtained from trials aligned on stimulus presentation of all groups of trials with activity that reached the 0.75 criterion and accurately reflected the beginning and end of the transition ($n = 108$). *C*: distributions of the time of the midway point in the transition obtained from trials aligned on stimulus presentation from the same groups of trials in *B* (shaded area, $n = 108$), and the TDTs obtained from trials aligned on stimulus presentation (- - -, $n = 150$) from all groups of trials with activity that reached the 0.75 criterion. *D*: distribution of the end of the transition aligned on stimulus presentation obtained from the same groups of trials in *B* ($n = 108$). *E*: distribution of saccade latencies on search trials obtained during the collection of the physiological data ($n = 6,250$). The last bin indicates the percentage of values that were >320 ms.

presentation. The midpoint values were slightly earlier than the DD_{stim} values (136 ± 2 ms) (t_{256} = 2.18, P = 0.03). The discrimination process was completed on average 142 ± 2 ms after stimulus presentation. Saccade latencies averaged 204 ± 1 ms. Notice that none of the distributions in Fig. 12, *A–D,* can directly predict the position or shape of the saccade latency distribution.

DISCUSSION

Previous work has quantified the time course of visual selection in single cells (Chelazzi et al. 1993; Lamme 1995; Motter 1994a,b; Oram and Perrett 1992; Shadlen and Newsome 1996). But this is the first study to relate the time course of a visual discrimination process at the single-cell level to the latency of a behavioral outcome on the basis of that discrimination, in this case a saccade to a target among distractors in a popout search display. This investigation yielded two main findings from macaque FEF, an area that in general terms converts the product of visual processing into a command to move the eyes (Bruce 1990; Goldberg and Segraves 1989; Schall 1991c, 1995). First, the visual response latencies of FEF cells did not differ for the target presented alone or with distractors, or for the distractors in a search array. Second, for most visually responsive cells, the time of target discrimination was more closely related to the time of sensory input than to the time of motor output. This is the first demonstration at the single-neuron level of an explicit dissociation between perceptual processing and response generation.

Time course of visual search target discrimination

To assure accuracy, a target must be located before a saccade can be generated to shift gaze (e.g., Viviani and Swensson 1982). Our results indicate the following sequence of events in the activity of FEF neurons that underlie the performance of a simple popout visual search discrimination task based on color or form differences. Beginning ~40 ms after the appearance of the search display, a population of neurons in FEF becomes activated by visual afferents. By 70 ms after stimulus presentation, most visually responsive FEF cells have responded. The discrimination process is well underway by 100 ms after the appearance of the visual search stimulus array. The reliability of the discrimination increases so that by 130 ms after the presentation of the search array the pattern of neural activity across FEF can reliably differentiate the target from the distractors. This transition in the pattern of activity is complete by ~140–160 ms after stimulus presentation. In other work we have found that the activity of presaccadic movement cells in FEF begins ~100 ms before saccades, and when their activity grows to a particular threshold a saccade is committed (Hanes et al. 1995; Hanes and Schall 1996). Thus our data indicate that at least two different stages of processing, target discrimination and response preparation, are reflected in the activation of neurons in FEF. Saccades to the target are produced as early as 110 ms to as late as 530 ms after stimulus appearance. On average, saccades to the target are produced ~200 ms after search array presentation.

The time of target discrimination was found to be delayed, on average, ~70 ms from the visual latency of FEF neurons. The discriminations used in this study are based on color and form information that is carried mainly in the longer-latency parvocellular stream and is processed through the ventral visual processing pathways (De Yoe and Van Essen 1988; Merigan and Maunsell 1993; Schiller and Logothetis 1990). A hypothesis we are currently testing is whether TDTs will be earlier if the search array is defined by motion differences.

The time course of the target discrimination process we measured in FEF is comparable with values obtained in previous studies. Luck and Hillyard (1994) have described the time course of discrimination during popout search in human subjects with the use of event-related potentials and found evidence of target discrimination over frontal lobe as early as 175 ms after stimulus presentation. Numerous studies have recorded neural activity under conditions in which the visual responses of neurons are modulated by visual context or task requirements in macaque V1 (Haenny and Schiller 1988; Knierim and Van Essen 1992; Lamme 1995; Motter 1993), V4 (Fischer and Boch 1985; Haenny and Schiller 1988; Haenny et al. 1988; Moran and Desimone 1985; Motter 1993, 1994a,b; Mountcastle et al. 1987), and further along the temporal (Chelazzi et al. 1993; Oram and Perrett 1992) and parietal (Shadlen and Newsome 1996) visual processing streams. Some of these studies have analyzed the time course of the discrimination process and found signals reflecting visual selection from 90 to 175 ms after stimulus presentation (Chelazzi et al. 1993; Lamme 1995; Motter 1994a,b; Oram and Perrett 1992). However, these times were obtained with the use of population averages, which precludes an analysis of the variability across neurons and, more importantly, prevents investigations of relationships between the time course of differentiation of neuronal activity and the timing of behavior such as saccade latency.

A long standing issue in neuroscience involves the extent to which visual processing is serial and hierarchical versus simultaneous and parallel. Two possibilities arise from the observation that studies across multiple brain areas by several investigators find comparable visual selection times. One possibility is that the sequence of visual processing is difficult to measure and will be evident only when differences on the order of milliseconds are resolved. Another possibility is that the visual system is a distributed network that transforms as a whole into a state representing visual selection with a common time course. That is, target selection is not localized temporally or anatomically. To effectively compare the timing of neural events across brain areas to evaluate these alternatives, it will be necessary to collect data across multiple brain areas with the use of common experimental designs and employ sensitive and reliable measurement techniques.

Processing stages

A useful approach toward understanding behavioral reaction times involves the notion of processing stages (Meyer et al. 1988; Miller 1988; Sternberg 1969; Taylor 1976). Previous efforts at subdividing reaction times had limited success because no reliable and sensitive index of the conclusion of processing of an intermediate stage had been identi-

fied. This work provides the first example, to our knowledge, of a neural signature that can be used to partition reaction time. We have distinguished two stages of processing. The interval of time we termed DD can be viewed as reflecting the perceptual stage of processing during which sensory processing discriminates stimuli and identifies the location of potential targets for saccades. The interval of time we termed the MD can be viewed as reflecting the motor stage of processing during which the command to produce the appropriate gaze shift arises and the movement is triggered. On the basis of our data showing that different components of reaction time can be measured in the activity of single neurons, we can advance our understanding of perceptuomotor systems by clarifying the relationships between successive stages, e.g., whether signals flow from one stage to the next in a discrete (Sternberg 1969), continuous (Eriksen and Schultz 1979), or some intermediate (Miller 1988) fashion. In other words, when and how does sensory processing influence response preparation?

The duration and variability in reaction time is commonly attributed to the time taken by covert decision processes (e.g., Carpenter and Williams 1995; Luce 1986). However, the nature of these decision processes is poorly specified or understood. The present data provide new information about the neural basis of the decision processes underlying saccade target discrimination and selection. We propose that the time at which the majority of visuomovement FEF neurons discriminates whether the target or a distractor is in their response field registers the outcome and conclusion of perceptual processing. At the moment indexed by TDT we would say that a potential target for a saccade has been discriminated, but it has not yet been selected. That is, the occurrence of TDT does not entail a commitment to execute a movement. In fact, we have found that most visuomovement neurons in FEF discriminate the salient oddball stimulus of the search array even if monkeys withhold a saccade (Bichot et al. 1996b; Thompson et al. 1997).

The discrimination of the potential target registered by FEF neurons represents more than the feature discrimination evidenced in visual cortical areas, because FEF neurons do not typically discriminate stimuli on the basis of visual features such as color, form, or motion except under specific training conditions (Bichot et al. 1996a). Instead, the pattern of activation of certain neurons in FEF may function as a saliency map, registering the location of stimuli that stand out as potential targets for saccades. One is then tempted to ask when the decision is made about which target will be selected. Our view is that target selection entails nothing more than the additional commitment of response preparation. The supposition of an intermediate decision stage seems unnecessary. We propose that response preparation is the growth of presaccadic movement activity in FEF (Bruce and Goldberg 1985; Hanes et al. 1995; Schall 1991b; Segraves 1992; Segraves and Goldberg 1987; Hanes and Schall 1996), which coincides with the presaccadic activation throughout the oculomotor system in a winner-take-all race. In other work we have found clear evidence that saccades are produced if and only if the movement activity of FEF neurons reaches a specific and constant threshold; the variability of reaction times is accounted for by variability in the rate of growth of premovement activation (Hanes and Schall 1996). The ultimate saccade is made into the movement field of the set of neurons in which the movement activity first reaches threshold. The reason that the duration of perceptual processing, indexed by DD, does not predict saccade latency is because in a simple visual discrimination task the response preparation stage of processing introduces most of the variability in the reaction time. It will likely be the case that as the discrimination task is made more difficult, additional delay and more variability will be introduced by the perceptual processing stage.

In conclusion, we must wonder why a gaze shift to a target is delayed after the perceptual discrimination has been completed. In the natural world, with its plethora of potential targets, the contents of the visual field and behavioral contingencies can change unpredictably. The delay intrinsic to saccade generation may provide the adaptive advantage of allowing for subsequent visual processing and cognitive factors to alter the choice of what to look at before an irrevocable commitment to move the eyes is made. Work in our laboratory is currently testing this hypothesis by exploring the neural processing underlying responses to unexpected changes in the visual array.

We thank O. Armstrong, K. Getz, and D. King for assistance with data acquisition and analysis.

This work was supported by National Eye Institute Grant R01 EY-08890 to J. Schall, NEI Grant F32 EY-06495 and a fellowship from the McDonnell-Pew Program in Cognitive Neuroscience to K. Thompson, and NEI Grants P30 EY-08126 and T32 EY-07135 to the Vanderbilt Vision Research Center.

Address for reprint requests: K. G. Thompson, Vanderbilt Vision Research Ctr., Dept. of Psychology, Wilson Hall, Vanderbilt University, Nashville, TN 37240.

Received 8 May 1996; accepted in final form 16 August 1996.

REFERENCES

AKAIKE, H. An information criterion. *Math. Sci.* 1: 5–9, 1976.

BATSCHELET, E. *Circular Statistics in Biology.* New York: Academic, 1981.

BICHOT, N. P., SCHALL, J. D., AND THOMPSON, K. G. Visual feature selectivity in frontal eye fields induced by experience in mature macaques. *Nature Lond.* 381: 697–699, 1996a.

BICHOT, N. P., THOMPSON, K. G., AND SCHALL, J. D. Dissociation of target selection from saccade planning in macaque frontal eye field. *Soc. Neurosci. Abstr.* 22: 1456, 1996b. .

BRADLEY, A., SKOTTUN, B. C., OHZAWA, I., SCLAR, G., AND FREEMAN, R. D. Visual orientation and spatial frequency discrimination: a comparison of single cells and behavior. *J. Neurophysiol.* 57: 755–772, 1987.

BRITTEN, K. H., SHADLEN, M. N., NEWSOME, W. T., AND MOVSHON, J. A. The analysis of visual motion: a comparison of neuronal and psychophysical performance. *J. Neurosci.* 12: 4745–4765, 1992.

BRUCE, C. J. Integration of sensory and motor signals for saccadic eye movements in the primate frontal eye fields. In: *Signal and Sense, Local and Global Order in Perceptual Maps,* edited by G. M. Edelman, W. E. Gall, and W. M. Cowan. New York: Wiley, 1990, p. 261–314.

BRUCE, C. J. AND GOLDBERG, M. E. Primate frontal eye fields. I. Single neurons discharging before saccades. *J. Neurophysiol.* 53: 603–635, 1985.

BRUCE, C. J., GOLDBERG, M. E., BUSHNELL, C., AND STANTON, G. B. Primate frontal eye fields. II. Physiological and anatomical correlates of electrically evoked eye movements. *J. Neurophysiol.* 54: 714–734, 1985.

CARPENTER, R. H. S. Oculomotor procrastination. In: *Eye Movements: Cognition and Visual Perception,* edited by D. F. Fisher, R. A. Monty, and J. W. Senders. Hillsdale, NJ: Erlbaum, 1981, p. 237–246.

CARPENTER, R. H. S. AND WILLIAMS, M. L. L. Neural computation of log likelihood in control of saccadic eye movements. *Nature Lond.* 377: 59–62, 1995.

CHELAZZI, L., MILLER, E. K., DUNCAN, J., AND DESIMONE, R. A neural

basis for visual search in inferior temporal cortex. *Nature Lond.* 363: 345–347, 1993.

COMMENGES, D. AND SEAL, J. The analysis of neuronal discharge sequences: change-point estimation and comparison of variances. *Stat. Med.* 4: 91–104, 1985.

COMMENGES, D. AND SEAL, J. The formulae-relating slopes, correlation coefficients and variance ratios used to determine stimulus- or movement-related activity. *Brain Res.* 383: 350–352, 1986.

CRIST, C. F., YAMASAKI, D. S., KOMATSU, H., AND WURTZ, R. H. A grid system and a microsyringe for single cell recording. *J. Neurosci. Methods* 26: 117–122, 1988.

DE YOE, E. A. AND VAN ESSEN, D. C. Concurrent processing streams in monkey visual cortex. *Trends Neurosci.* 11: 219–226, 1988.

EGAN, J. P. *Signal Detection Theory and ROC Analysis.* New York: Academic, 1975.

ERIKSEN, C. W. AND SCHULTZ, D. W. Information processing in visual search: a continuous flow conception and experimental results. *Percept. Psychophys.* 25: 249–263, 1979.

FISCHER, B. AND BOCH, R. Peripheral attention versus central fixation: modulation of the visual activity of prelunate cortical cells of the rhesus monkey. *Exp. Brain Res.* 345: 111–123, 1985.

GOLDBERG, M. E. AND BUSHNELL, M. C. Behavioral enhancement of visual responses in monkey cerebral cortex. II. Modulation in frontal eye fields specifically related to saccades. *J. Neurophysiol.* 46: 773–787, 1981.

GOLDBERG, M. E. AND SEGRAVES, M. A. The visual and frontal cortices. In: *The Neurobiology of Saccadic Eye Movements, Reviews of Oculomotor Research,* edited by R. H. Wurtz and M. E. Goldberg. New York: Elsevier, 1989, vol. 3, p. 283–313.

GREEN, D. M. AND SWETS, J. A. *Signal Detection Theory and Psychophysics.* New York: Wiley, 1966.

GUIDO, W., LU, S.-M., VAUGHAN, J. W., GODWIN, D. W., AND SHERMAN, S. M. Receiver operating characteristic (ROC) analysis in the cat's lateral geniculate nucleus during tonic and burst response mode. *Visual Neurosci.* 12: 723–741, 1995.

HAENNY, P. E., MAUNSELL, J. H. R., AND SCHILLER, P. H. State dependent activity in monkey visual cortex. II. Retinal and extraretinal factors in V4. *Exp. Brain Res.* 69: 245–259, 1988.

HAENNY, P. E. AND SCHILLER, P. H. State dependent activity in monkey visual cortex. I. Single cell activity in V1 and V4 on visual tasks. *Exp. Brain Res.* 69: 225–244, 1988.

HANES, D. P., AND SCHALL, J. D. Neural control of voluntary movement initiation. *Science Wash. DC* 274: 427–430, 1996.

HANES, D. P., THOMPSON, K. G., AND SCHALL, J. D. Relationship of presaccadic activity in frontal eye field and supplementary eye field to saccade initiation in macaque: Poisson spike train analysis. *Exp. Brain Res.* 103: 85–96, 1995.

KIM, H. AND CONNORS, B. Apical dendrites of the neocortex: correlation between sodium- and calcium-dependent spiking and pyramidal cell morphology. *J. Neurosci.* 13: 5301–5311, 1993.

KNIERIM, J. J. AND VAN ESSEN, D. C. Neuronal responses to static texture patterns in area V1 of the alert macaque monkey. *J. Neurophysiol.* 67: 961–980, 1992.

LAMME, V. A. F. The neurophysiology of figure-ground segregation in primary visual cortex. *J. Neurosci.* 15: 1605–1615, 1995.

LEVICK, W. R. AND ZACKS, J. L. Responses of cat retinal ganglion cells to brief flashes of light. *J. Physiol. Lond.* 206: 677–700, 1970.

LUCE, R. D. *Response Times: Their Role in Inferring Elementary Mental Organization.* New York: Oxford Univ. Press, 1986.

LUCK, S. J. AND HILLYARD, S. A. Electrophysiological correlates of feature analysis during visual search. *Psychophysiology* 31: 291–308, 1994.

MACMILLAN, N. A. AND CREELMAN, C. D. *Detection Theory: A User's Guide.* New York: Cambridge Univ. Press, 1991.

MASON, A., NICOLL, A., AND STRATFORD, K. Synaptic transmission between individual pyramidal neurons of the rat visual cortex in vitro. *J. Neurosci.* 11: 72–84, 1991.

MERIGAN, W. H. AND MAUNSELL, J. H. R. How parallel are the primate visual pathways? *Annu. Rev. Neurosci.* 16: 369–402, 1993.

MEYER, D. E., OSMAN, A. M., IRWIN, D. E., AND YANTIS, S. Modern mental chronometry. *Biol. Psychol.* 26: 3–67, 1988.

MILLER, J. O. Discrete and continuous models of human information processing: theoretical distinctions and empirical results. *Acta Physiol.* 67: 1–67, 1988.

MORAN, J. AND DESIMONE, R. Selective attention gates visual processing in the extrastriate cortex. *Science Wash. DC* 229: 782–784, 1985.

MOTTER, B. C. Focal attention produces spatially selective processing in visual cortical areas V1, V2, and V4 in the presence of competing stimuli. *J. Neurophysiol.* 70: 909–919, 1993.

MOTTER, B. C. Neural correlates of attentive selection for color or luminance in extrastriate area V4. *J. Neurosci.* 14: 2178–2189, 1994a.

MOTTER, B. C. Neural correlates of feature selective memory and pop-out in extrastriate area V4. *J. Neurosci.* 14: 2190–2199, 1994b.

MOUNTCASTLE, V. B., MOTTER, B. C., STEINMETZ, M. A., AND SESTOKAS, A. K. Common and differential effects of attentive fixation on the excitability of parietal and prestriate (V4) cortical visual neurons in the macaque monkey. *J. Neurosci.* 7: 2239–2255, 1987.

ORAM, M. W. AND PERRETT, D. I. Time course of neural responses discriminating different views of the face and head. *J. Neurophysiol.* 68: 70–84, 1992.

PARTHASARATHY, H. B., SCHALL, J. D., AND GRAYBIEL, A. M. Distributed but convergent ordering of corticostriatal projections: analysis of the frontal eye field and the supplementary eye field in the macaque monkey. *J. Neurosci.* 12: 4468–4488, 1992.

PRESS, W. H., FLANNERY, B. P., TEUKOLSKY, S. A., AND VETTERLING, W. T. *Numerical Recipes in C.* Cambridge, UK: Cambridge Univ. Press, 1988.

PREUSS, T. M. AND GOLDMAN-RAKIC, P. S. Myelo- and cytoarchitecture of the granular frontal cortex and surrounding regions of the strepsirhine primate *Galago* and the anthropoid primate *Macaca. J. Comp. Neurol.* 310: 429–474, 1991.

RICHMOND, B. J. AND OPTICAN, L. M. Temporal encoding of two-dimensional patterns by single units in primate inferior temporal cortex. II. Quantification of response waveform. *J. Neurophysiol.* 57: 147–161, 1987.

RICHMOND, B. J., OPTICAN, L. M., AND SPITZER, H. Temporal encoding of two-dimensional patterns by single units in primate primary visual cortex. I. Stimulus response relations. *J. Neurophysiol.* 64: 351–369, 1990.

SAYER, R. J., FRIEDLANDER, M. J., AND REDMAN, S. J. The time course and amplitude of EPSPs evoked at synapses between pairs of CA3/CA1 neurons in the hippocampal slice. *J. Neurosci.* 10: 826–836, 1990.

SCHALL, J. D. Neuronal activity related to visually guided saccadic eye movements in the supplementary motor area of rhesus monkeys. *J. Neurophysiol.* 66: 530–558, 1991a.

SCHALL, J. D. Neuronal activity related to visually guided saccades in the frontal eye fields of rhesus monkeys: comparison with supplementary eye fields. *J. Neurophysiol.* 66: 559–579, 1991b.

SCHALL, J. D. Neuronal basis of saccadic eye movements. In: *The Neural Basis of Visual Function,* edited by A. G. Leventhal. In: *Vision and Visual Dysfunction,* edited by J. Cronly-Dillon. London: Macmillan, 1991c, vol. 4, p. 388–442.

SCHALL, J. D. Neural basis of saccade target selection. *Rev. Neurosci.* 6: 63–85, 1995.

SCHALL, J. D. AND HANES, D. P. Neural basis of saccade target selection in frontal eye field during visual search. *Nature Lond.* 366: 467–469, 1993.

SCHALL, J. D., HANES, D. P., THOMPSON, K. G., AND KING, D. J. Saccade target selection in frontal eye field of macaque. I. Visual and premovement activation. *J. Neurosci.* 15: 6905–6918, 1995a.

SCHALL, J. D., MOREL, A., KING, D. J., AND BULLIER, J. Topography of visual cortical afferents to frontal eye field in macaque: functional convergence and segregation of processing streams. *J. Neurosci.* 15: 4464–4487, 1995b.

SCHILLER, P. H. AND LOGOTHETIS, N. K. The color-opponent and broad-band channels of the primate visual system. *Trends Neurosci.* 13: 392–398, 1990.

SEGRAVES, M. A. Activity of monkey frontal eye field neurons projecting to oculomotor regions of the pons. *J. Neurophysiol.* 68: 1967–1985, 1992.

SEGRAVES, M. A. AND GOLDBERG, M. E. Functional properties of corticotectal neurons in the monkey's frontal eye fields. *J. Neurophysiol.* 58: 1387–1419, 1987.

SEGRAVES, M. A. AND PARK, K. The relationship of monkey frontal eye field activity to saccade dynamics. *J. Neurophysiol.* 69: 1880–1889, 1993.

SHADLEN, M. N. AND NEWSOME, W. T. Motion perception: seeing and deciding. *Proc. Natl. Acad. Sci. USA* 93: 628–633, 1996.

STANTON, G. B., DENG, S. Y., GOLDBERG, M. E., AND MCMULLEN, N. T. Cytoarchitectural characteristics of the frontal eye fields in macaque monkeys. *J. Comp. Neurol.* 271: 493–506, 1989.

STERNBERG, S. The discovery of processing stages: extensions of Donders' method. *Acta Psychol.* 30: 276–315, 1969.

TAYLOR, D. Stage analysis of reaction time. *Psychol. Bull.* 83: 161–191, 1976.

THOMPSON, K. G., HANES, D. P., AND SCHALL, J. D. Timecourse of target selection in macaque frontal eye field during visual search. *Soc. Neurosci. Abstr.* 21: 1270, 1995.

THOMSON, A., DEUCHARS, J., AND WEST, D. Single axon excitatory postsynaptic potentials in neocortical interneurons exhibit pronounced paired pulse facilitation. *Neuroscience* 54: 347–360, 1993a.

THOMSON, A., DEUCHARS, J., AND WEST, D. Large, deep layer pyramid-pyramid single axon EPSPs in slices of rat motor cortex display paired pulse and frequency-dependent depression, mediated presynaptically and self-facilitation, mediated postsynaptically. *J. Neurophysiol.* 70: 2354–2369, 1993b.

TOLHURST, D. J., MOVSHON, J. A., AND DEAN, A. F. The statistical reliability of signals in single neurons in cat and monkey visual cortex. *Vision Res.* 23: 775–785, 1983.

VIVIANI, P. AND SWENSSON, R. G. Saccadic eye movements to peripherally discriminated visual targets. *J. Exp. Psychol. Hum. Percept. Perform.* 8: 113–126, 1982.

VOGELS, R. AND ORBAN, G. A. How well do response changes of striate neurons signal differences in orientation: a study in the discriminating monkey. *J. Neurosci.* 10: 3543–3558, 1990.

VON BONIN, G. AND BAILEY, P. *The Neocortex of Macaca mulatta.* Urbana, IL: Univ. of Illinois, 1947.

WAITZMAN, D. M., MA, T. P., OPTICAN, L. M., AND WURTZ, R. H. Superior colliculus neurons mediate the dynamic characteristics of saccades. *J. Neurophysiol.* 66: 1716–1737, 1988.

WALKER, A. E. A cytoarchitectural study of the prefrontal area of the macaque monkey. *J. Comp. Neurol.* 73: 59–86, 1940.

ZOHARY, E., HILLMAN, P., AND HOCHSTEIN, S. Time course of perceptual discrimination and single neuron reliability. *Biol. Cybern.* 62: 475–486, 1990.